Hittite Journal of Science and Engineering, 2023, 10 (1) 1-9
ISSN NUMBER: 2149-2123
DOI: 10.17350/HJSE19030000285

Performance Analysis of Fresnel Lens Driven Hot Water/ Steam Generator for Domestic and Industrial Use: A CFD Research

Pinar Mert Cuce[1] **Erdem Cuce**[2,3]
[1] Recep Tayyip Erdogan University, Department of Architecture, Rize, Turkey
[2] Low/Zero Carbon Energy Technology Laboratory (L/ZCarE), Rize, Turkey
[3] Recep Tayyip Erdogan University, Department of Mechanical Engineering, Rize, Turkey

ABSTRACT

This study presents the design, manufacture, and thermal performance analysis of a Fresnel lens-driven hot water/steam generator. The designed system is suitable for domestic and industrial hot water/steam usage and can be easily scaled up to meet different capacity needs. In the first step of the research, the thermal behavior of the cast plate heat exchanger driven by a Fresnel lens with a concentration ratio of 100 is investigated at different working fluid velocities (0.6, 0.8, 1.0, 1.5 and 2.0 m/s) and at different absorber surface temperatures. The outlet temperature of working fluid from the cast plate heat exchanger is determined through a 3D CFD model for each case. The capacity of the steam generator for different operating times (h = 1, 2 and 3 hours) is also evaluated. The highest working fluid temperature at the outlet of the heat exchanger is 914.8 °C for T_{cp} = 1000 °C and V_{wf} = 0.6 m/s. On the other hand, the lowest temperature is observed as 424.7 °C for T_{cp} = 700 °C and V_{wf} = 2.0 m/s. The steam capacity of the system for h = 3 hours is determined as 1696.5 and 508.9 kg in the best (V_{wf} = 2.0 m/s) and worst cases (V_{wf} = 0.6 m/s), respectively.

Keywords:
Solar collector; Fresnel lens; Steam generator; Domestic hot water; Thermal performance

Article History:
Received: 2022/03/23
Accepted: 2023/01/27
Online: 2023/03/31

***Correspondence to**: Pınar Mert Cüce,*
Recep Tayyip Erdoğan University,
Department of Artitecture, Rize, Turkey
E-Mail:pinarmertcuce@erdogan.edu.tr

INTRODUCTION

Solar energy is the most important sustainable and accessible natural resource that significantly reduces the use of non-renewable energy resources [1]. Among the solar energy applications, concentrated solar collectors (CSCs) draw attention as an effective and efficient system for various applications such as heating, cooling, energy production, desalination, chemical processes, etc. [2]. CSCs are the systems that convert sunlight into heat and raise the temperature well above the ambient temperature [3]. Among the CSCs, Fresnel lenses or collectors, which enable high amounts of useful heat generation up to 500 °C, stand out as a cost-effective technology and are frequently studied by scientists in the literature [4].

There has been a great interest in Fresnel lens-based CSCs in recent years. In this context, there are plenty number of experimental studies in the literature to observe reliable and accurate performance assessments of this renewable energy technology. For instance, Zhai et al. [5] conducted an experimental study to investigate the thermal efficiency of a CSC using a linear Fresnel lens. For this purpose, they developed a linear Fresnel lens concentrator using an evacuated glass tube as the absorber. According to the test results, when the working fluid temperature in the system is 90 °C thermal efficiency is found to be about 50%. The results also indicate that the heat loss coefficient (HLC) was determined to be 0.578 W/m^{2}K. Perini et al. [6] investigated a novel CSC driven by a Fresnel lens with dual-axis solar tracking experimentally and theoretically. They proposed a mathematical model and developed an experimental test rig in Bourne, UK to achieve the performance characteristics of the innovative CSC unit. The research findings showed that the collector's maximum efficiency is 20%. It was also observed that the optical losses in the CSC system constitute 47% of the total energy losses. In another study, Ma et al. [7] studied the shape effect of a curved-Fresnel lens to enhance the transmissivity. They analyzed polarized light and p-polarized light separately. According to their study, p-polarized light has higher transmittance than s-polarized light, and the total transmittance increases with the decrease of incidence angle.

Lin et al. [8] conducted a comprehensive analysis of a linear Fresnel lens-assisted CSC with a cavity receiver. They used various cavity receivers to evaluate the proposed CSC's optical and thermal performance. The highest optical efficiency was observed to be 81.2% for the triangular cavity receiver. They also reported that the thermal efficiency is about 30% at 120 °C. Xie et al. [9] analyzed the thermal behavior of a CSC driven by a Fresnel lens with different cavity receivers. The collector heat removal factor (HRF) and the collector efficiency were compared for various cavity receiver designs both experimentally and theoretically. The results indicated that the triangular cavity receiver had the best thermal performance. For the fluid temperature of 90 °C at the inlet, the greatest HRF was determined to be 0.866 with an efficiency factor of 0.87. On the other hand, when the inlet condition was changed to 150 °C, HRF and efficiency factor reduce to 0.824 and 0.843, respectively. It was also reported that the HLC for 90 and 150 °C inlet conditions were 12 and 24 W/m^{2}K, respectively. Wu et al. [10] analyzed the performance of a solar desalination system having a cylindrical Fresnel lens. The system includes humidification and dehumidification units and was integrated with a Fresnel lens collector for enhanced water productivity. An experimental analysis was carried out with the justification of theoretical results. The findings revealed that the freshwater productivity of the Fresnel lens-driven CSC was about 3.4 kg/h for the average solar radiation of 867 W/m^2. Beltagy et al. [11] conducted an experimental and theoretical analysis to observe the performance of a Fresnel type CSC. According to their study, the thermal daily efficiency was measured to be more than 40% for the installed thermal prototype capacity of 250 kW.

Asrori et al. [12] investigated the steam generation performance of a Fresnel lens concentrator for distinct geometrical concentration ratios. For this purpose, they proposed a design with conical cavity receivers having different geometric ratios, and compared the thermal efficiencies. According to the experimental results, about 1.37 MJ of steam latent thermal energy per cycle can provide a valuable efficiency of 31.81% for large receivers. For the small conical receivers with an insulator, steam latent thermal energy and useful efficiency are observed as 579.17 kJ per cycle and 33.31%, respectively. They recommended that using small receivers is more beneficial than large receivers thanks to their advantages like higher efficiency, short cycle times and low saturation pressure. In another study, Vega [13] examined the cost-effectiveness and feasibility of a small-scale Fresnel CSC. The research aimed to determine the thermal performance of different applications like solar cooking, boiling water, and autoclaves. Experimental and theoretical results demonstrated that the solar thermal energy obtained from the said system was sufficient for various applications. Also, efficiency was measured at over 50% for the boiling water application, which is noteworthy. Zulkifle et al. [14] presented an analysis of the thermal performance assessment of solar thermal collectors with Fresnel lens or glass. They used a theoretical approach to estimate the solar collectors' thermal efficiencies for any mass flow rate value. The research was conducted for glass and Fresnel lens under the same conditions and results are compared. The results revealed that for the same operation conditions, the efficiency of a Fresnel lens-driven solar collector can reach 71.18%, while the efficiency is 54.10% with glass. Ma et al. [15] presented an optimization study for a cylindrical Fresnel lens application to validate the thermal and optical performance of a solar steam generation system. They built a solar concentrator with a 20 m^2 surface area and carried out tests under 0.2 and 0.5 MPa operating pressures. The intercept efficiency was determined to be about 63%.

When the Fresnel lens-based CSCs in recent years are investigated in detail, it can be concluded that a great majority of the works merely aim to evaluate the thermal performance figures notably system efficiency for a particular concentration ratio (CR) and system design. In Fresnel lens-based CSCs, heat exchanger design is vital for system efficiency. To determine the thermal behavior of the system for different climatic and operating conditions is therefore essential. Within the scope of this research, a unique Fresnel lens-driven hot water/steam generator for domestic and industrial use is introduced. The proposed system has already been patented by the authors of this manuscript through document no: 2015/15776 by the Turkish Patent and Trademark Office. As the first step of this research, Fresnel lens-driven hot water/steam generator is numerically investigated for various climatic and operating conditions. The outlet temperature of the working fluid is determined as a function of cast plate temperature and working fluid velocity. The steam capacity of the proposed system is also obtained as a function of operation time and velocity of working fluid. The numerical calculations are conducted through a reliable and well-known commercial CFD software ANSYS FLUENT [16]. In the second step of the study, the numerical study was confirmed by an experimental study.

The main purpose of this study is to observe the collector outlet temperature values for different fluid velocities under different solar radiation and ambient temperature conditions. Determining an optimum Concentration Ratio value is not the main purpose of this study.

SYSTEM DESCRIPTION

Fresnel lens-driven hot water/steam generator developed for domestic and industrial use within the scope of this research is shown in Fig. 1. The present invention consists of a Fresnel lens-driven CSC unit, a coil-type heat exchanger with single and double pass design options placed at the focal point of the concentrating unit, a sing-

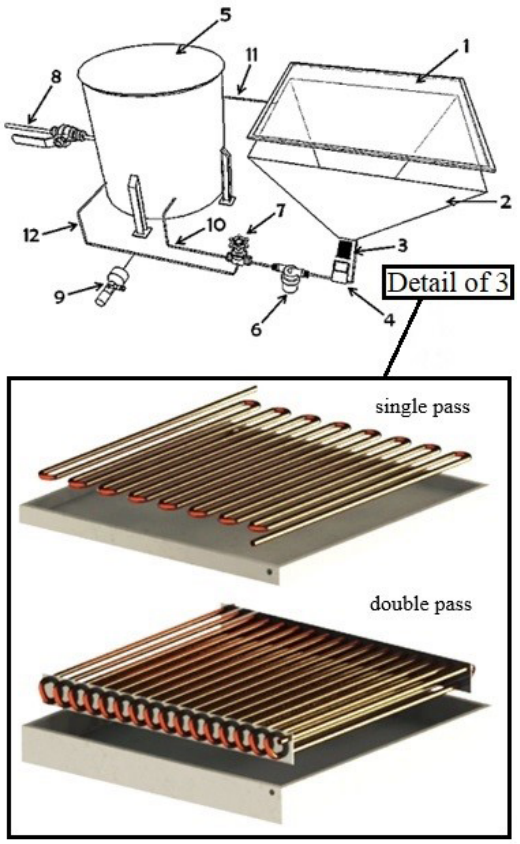

Figure 1. Schematic of Fresnel lens driven novel hot water/steam generator; (1) Fresnel lens, (2) chimney hood, (3) coil type heat exchanger with single and double pass design, (4) ceramic shell apparatus, (5) PCM and vacuum-walled water tank, (6) pump, (7) thermostatic valve, (8) valve, (9) temperature sensor, (10) cold water line, (11) hot water line, (12) temperature control line.

le inlet and single outlet shell apparatus on which the said heat exchanger is mounted, which quickly and effectively supplies the domestic hot water need of the buildings. An innovative collector system consists of a phase change material (PCM) and a vacuum-walled water tank, where heat energy is stored with minimal energy loss.

The solar radiation on the Fresnel lens (1) is concentrated at the focal point depending on the Concentration Ratio (CR) of the concentrator, which is defined as the aperture area divided by the receiver/absorber area of the collector (1). A square-bottom, truncated pyramid hood (2) with optimized focus according to the Fresnel lens (1) to be used is mounted on the concentrator (1) so that the concentrated solar energy does not pose any danger to both the user and the system elements. High and intense solar energy, which is transferred to the focal point safely and without loss, drives the heat exchanger (3) with a single or double pass design option, which is made of material with high melting temperature and thermal conductivity. The said heat exchanger (3) with a coil-type design is placed inside a shell apparatus (4) produced from a material with very high thermal conductivity. The said shell apparatus (4) is connected to two water lines, one inlet and one outlet. The cold water drawn from a water tank (5) using the pump (6) comes to the heat exchanger (3) with a single or double pass design. Thanks to the heat exchanger's very high heat transfer surface area (3) with the coil design and the concentrated solar energy, the heated water returns to the tank again. The water tank (5) contains PCM on all surfaces and a very thin vacuum layer around it so that the water does not lose its energy. The water temperature in the discharge line (10) is regularly controlled with the temperature sensor (9) and the collection line (11) is closed with the temperature-sensitive valve (7) when necessary. The temperature-sensitive valve (7) is connected to the tank (5) via the temperature control line (12) and automatically cuts off the water flow according to the notification from the temperature sensor (9). The water level in the tank (5) is kept constant by a controlled valve (8).

CFD Research and Model Details

Firstly, a spiral-shaped cylindrical copper pipe was placed inside the rectangular prism-shaped chamber. One surface of the chamber was kept at a constant temperature, and water with a different flow rate was supplied from the inlet side of the copper pipe. Simulations were repeated for different surface temperatures and water flow rates.

In the system, one surface of the chamber was kept at a constant temperature and the other five surfaces were adiabatic, the copper pipe inlet is defined as velocity inlet and its outlet as pressure outlet. Convection boundary condition was applied between the copper pipe and the water, which is the working fluid. The pressure-velocity coupling scheme was determined as coupled. On the other hand, for the numerical discretization, the gradient was based on the least squares cell and the pressure, momentum and energy were preferred as the second order upwind. First order upwind option was used for turbulent kinetic energy and dispersion rate. 10^{-6} was considered sufficient as a convergence criterion.

Thermal performance analysis of a Fresnel lens-driven hot water/steam generator was conducted for various operating conditions. Thermal behavior of the cast plate heat exchanger assisted by a Fresnel lens with a concentration ratio of 100 was analyzed at different working fluid velocities (0.6, 0.8, 1.0, 1.5 and 2.0 m/s) and different absorber surface temperatures (300, 400, 500, 700, 800, 900 and 1000°C). The reason for studying a wide range of cast plate temperature is to examine the performance figures of the system under different concentration ratios (CRs). Lower CRs are expected to yield lower cast plate temperatures from 300 to 500 °C whereas it would be possible to achieve greater temperatures up to 1000 °C with higher CRs. The working fluid's

inlet temperature was kept constant at 15 °C for a realistic assumption. On the other hand, the outlet temperature of working fluid from the cast plate heat exchanger was determined through a 3D CFD model for each case. The capacity of the steam generator for different operating times (h = 1, 2 and 3 hours) was also evaluated in this numerical research.

Conservation equations were solved simultaneously in simulations and can be given as [17]:

Continuity equation:

$$\frac{\partial(\rho V_r r)}{r\partial r}+\frac{\partial(\rho V_z)}{\partial z}dr+\frac{\partial(\rho V_\theta)}{r\partial\theta}=0 \quad (1)$$

Momentum equation:

$$\rho\left(\frac{\partial V_r}{\partial t}+V_r\frac{\partial V_r}{\partial r}+\frac{V_\theta}{r}\frac{\partial V_r}{\partial\theta}+V_z\frac{\partial V_r}{\partial z}-\frac{V_\theta^2}{r}\right)= -\frac{\partial p}{\partial r}+\mu\left(\begin{array}{l}\frac{\partial}{\partial r}\left[\frac{1}{r}\frac{\partial}{\partial r}(rV_r)\right]+\\ \frac{1}{r^2}\frac{\partial^2 V_r}{\partial\theta^2}+\frac{\partial^2 V_r}{\partial z^2}-\frac{2}{r^2}\frac{\partial V_\theta}{\partial\theta}\end{array}\right)+\rho g_r \quad (2)$$

$$\rho\left(\frac{\partial V_\theta}{\partial t}+V_r\frac{\partial V_\theta}{\partial r}+\frac{V_\theta}{r}\frac{\partial V_\theta}{\partial\theta}+V_z\frac{\partial V_\theta}{\partial z}+\frac{V_\theta^2}{r}\right)= -\frac{1}{r}\frac{\partial p}{\partial\theta}+\mu\left(\begin{array}{l}\frac{\partial}{\partial r}\left[\frac{1}{r}\frac{\partial}{\partial\theta}(rV_\theta)\right]+\\ \frac{1}{r^2}\frac{\partial^2 V_\theta}{\partial\theta^2}+\frac{\partial^2 V_\theta}{\partial z^2}+\frac{2}{r^2}\frac{\partial V_r}{\partial\theta}\end{array}\right)+\rho g_\theta \quad (3)$$

$$\rho\left(\frac{\partial V_z}{\partial t}+V_r\frac{\partial V_z}{\partial r}+\frac{V_\theta}{r}\frac{\partial V_z}{\partial\theta}+V_z\frac{\partial V_r}{\partial z}\right)= -\frac{\partial p}{\partial z}+\mu\left(\begin{array}{l}\frac{1}{r}\frac{\partial}{\partial r}\left(r\frac{\partial V_z}{\partial r}\right)+\\ \frac{1}{r^2}\frac{\partial^2 V_z}{\partial\theta^2}+\frac{\partial^2 V_z}{\partial z^2}\end{array}\right)+\rho g_z \quad (4)$$

Energy equation:

$$\frac{1}{k}\frac{\partial}{\partial r}\left(kr\frac{\partial T}{\partial r}\right)+\frac{1}{r^2}\frac{\partial}{\partial\varphi}\left(kr\frac{\partial T}{\partial\varphi}\right)+ \frac{\partial}{\partial z}\left(k\frac{\partial T}{\partial z}\right)+q_v=\rho c_p\frac{\partial T}{\partial t} \quad (5)$$

Table 1. Calculation of Re number for analysis.

	ρ (kg/m³)	V(m/s)	D (m)	μ (kg/m.s)	Re number
1	998.95	0.6	9x10⁻³	1.12x10⁻³	4816.36
2	998.95	2	9x10⁻³	1.12x10⁻³	16054.55

When the flow characteristics in the analysis are examined, it is clear that there is an internal flow problem. The critical Re number for inflow is 2300. Since the Re value calculated in the simulations is much higher than the critical value, all flows are turbulent. Calculation details are given in Table 1.

It is seen from Table 1 that the Re number is greater than the critical value when calculated for the maximum and minimum water flow rate. RNG k-e turbulence model is used as turbulence model in the research. The corresponding turbulence equations are as follows:

$$\frac{\partial}{\partial x_i}(\rho k u_i)=\frac{\partial}{\partial x_j}\left[\alpha_k\mu_{eef}\frac{\partial k}{\partial x_j}\right]+G_k+G_b+\rho\varepsilon-Y_m+S_k \quad (6)$$

$$\frac{\partial}{\partial x_i}(\rho\varepsilon u_i)=\frac{\partial}{\partial x_i}\left[\alpha_\varepsilon\mu_{eef}\frac{\partial\varepsilon}{\partial x_j}\right]+ C_{1\varepsilon}\frac{\varepsilon}{k}(G_k+C_{3\varepsilon}G_b)-C_{2\varepsilon}\rho\frac{\varepsilon^2}{k}-R_e+S_\varepsilon \quad (7)$$

Validation of the Designed Model

First of all, a Mesh-independent solution is obtained through the CFD analyses carried out at different cell numbers, and optimum mesh was achieved for a cell count which is greater than 500k as shown in Table 2 and view in Fig. 2. Since the change in the number of 530000 cells is negligible, the relevant cell number is considered sufficient.

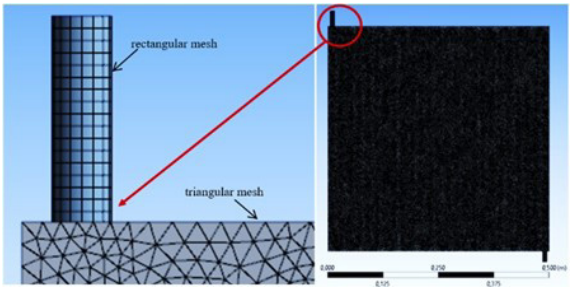

Figure 2. Mesh structure adopted in the CFD analyses

Table 2. Mesh-independent study for CFD model.

Elements Number	Average outlet temperature (ºC)	% change
241000	37.921	-
354000	37.894	0.071
530000	37.893	0.00263

In the absence of a significant change in temperature difference in response to the change in element number, the element number can be considered sufficient for accurate and consistent analysis results [18]. As seen in Fig. 3, while the number of elements increased from 354000 to 530000, the change in temperature has been observed as only 0.00263%. This confirms that mesh-independent solution is achieved for >500k cell counts in which rectangular mesh is

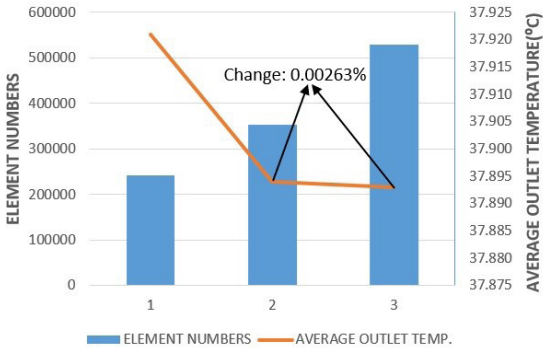

Figure 3. Mesh-independent solution results

preferred at the spiral coils and triangular mesh at the cast plate.

In the experimental study, the initial temperature of the water entering the heat exchanger is 19.3 °C. The experimental setup is shown in Fig. 4.

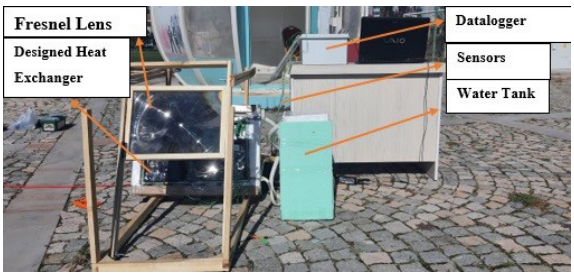

Figure 4. Experimental setup of the designed system

In the tests carried out using a 10-liter tank, the water temperature was measured as 37.4 °C at the exit of the heat exchanger after 2.5 hours. The results obtained from the experimental study are shown in Fig. 5. As seen in Fig. 6, the exit temperature was observed as 37.950 °C in the results obtained from the CFD study.

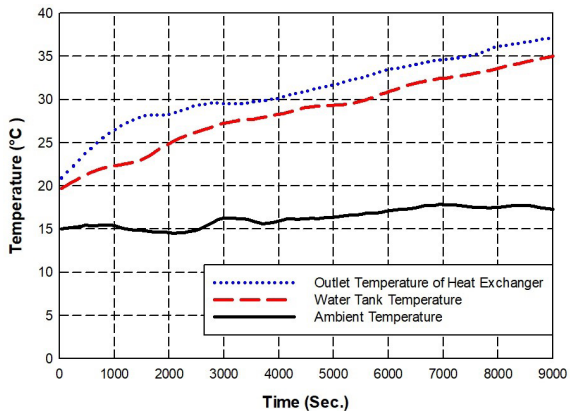

Figure 5. The results obtained from the experimental study

RESULTS AND DISCUSSION

The velocity of working fluid is a significant parameter in the design in terms of performance and capacity. For V_{wf}= 1 m/s, a promising hot water/steam capacity is expected from the design through the preliminary analyses when a pipe diameter (D) of 9 mm was considered. In this respect, for the said velocity of working fluid, temperature profiles in the coil-type heat exchanger are achieved for a wide range of cast plate temperatures (T_{cp}) from 300 to 1000°C as shown in Figure 7 and Fig. 5.

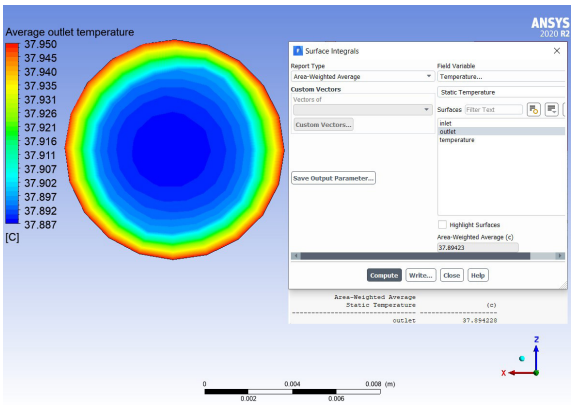

Figure 6. CFD validation results

The important parameters affecting the outlet temperature are the fluid inlet velocity and the plate surface temperature. As seen in Fig. 7 and Fig. 8 for the same fluid inlet velocity, increasing the plate surface temperature directly increases the outlet temperature. At 500 °C plate surface temperature, the outlet temperature is observed as 405.9°C, and when the plate surface temperature was doubled to 1000 °C, it is seen that the outlet temperature is 804.9°C. It is observed that the outlet temperature does not reach two times.

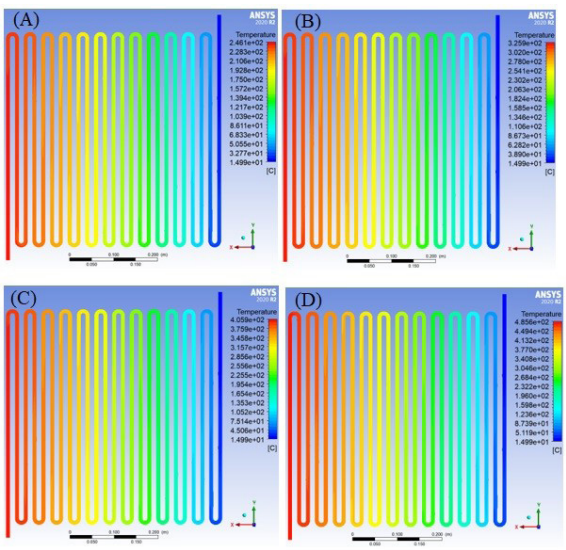

Figure 7. Static contours of temperature in the coil type heat exchanger for T_{in} = 15 °C and V_{wf} = 1 m/s: a) T_{cp} = 300 °C, b) T_{cp} = 400 °C, c) T_{cp} = 500 °C and d) T_{cp} = 600 °C.

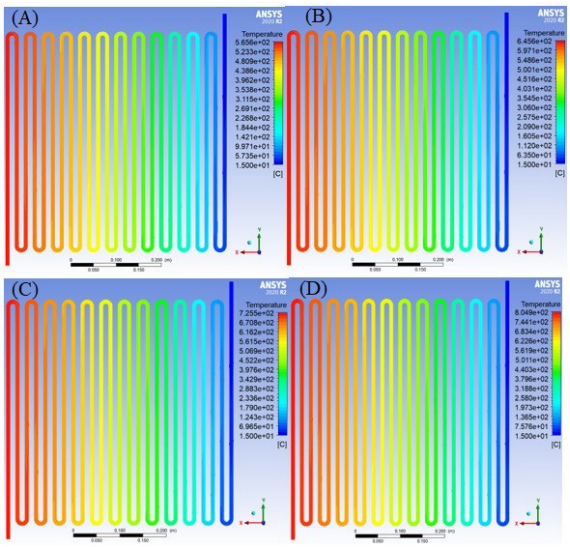

Figure 8. Static contours of temperature in the coil type heat exchanger for T_{in} = 15 °C and V_{wf} = 1 m/s: a) T_{cp} = 700 °C, b) T_{cp} = 800 °C, c) T_{cp} = 900 °C and d) T_{cp} = 1000 °C.

The effect of the increase in the plate surface temperature on the outlet temperature for a constant fluid inlet temperature is clearly seen in the static contours of temperature. Another parameter that affects the outlet temperature, such as the plate surface temperature, is the fluid inlet velocity. The temperature contours obtained by changing the plate surface temperature between 700-1000 °C for the fluid inlet velocity of 0.6 m/s, respectively, are given in Fig. 9. Similarly, the temperature contours achieved by making the fluid inlet velocity 0.8 m/s for the same temperature range are given in Fig. 10.

It is seen that the fluid inlet velocity has a significant effect on the outlet temperature when compared to the same

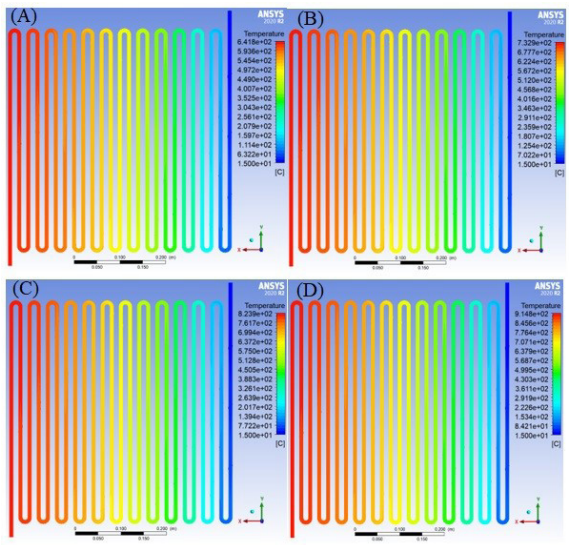

Figure 9. Static contours of temperature in the coil type heat exchanger for T_{in} = 15 °C and V_{wf} = 0.6 m/s: a) T_{cp} = 700 °C, b) T_{cp} = 800 °C, c) T_{cp} = 900 °C and d) T_{cp} = 1000 °C.

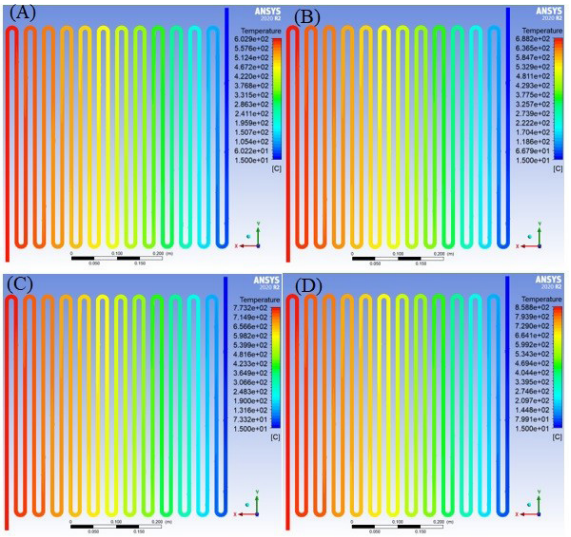

Figure 10. Static contours of temperature in the coil type heat exchanger for T_{in} = 15 °C and V_{wf} = 0.8 m/s: a) T_{cp} = 700 °C, b) T_{cp} = 800 °C, c) T_{cp} = 900 °C and d) T_{cp} = 1000 °C.

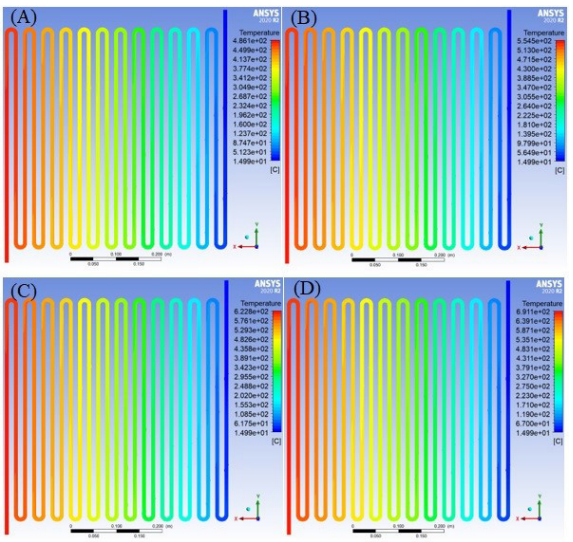

Figure 11. Static contours of temperature in the coil type heat exchanger for T_{in} = 15 °C and V_{wf} = 1.5 m/s: a) T_{cp} = 700 °C, b) T_{cp} = 800 °C, c) T_{cp} = 900 °C and d) T_{cp} = 1000 °C.

plate surface temperatures. At 0.8 m/s fluid inlet velocity, the outlet temperature is observed as 858.8 °C at 1000 °C plate surface temperature, and when the fluid inlet velocity is 0.6 m/s, the outlet temperature is 914.8 °C for the same plate surface temperature. It was understood that despite a 25% decrease in fluid inlet velocity, the outlet temperature (for a constant plate temperature of 1000 °C) increases by 6.5%.

It is seen that when the fluid inlet velocity increases, the outlet temperature decreases for the same plate surface temperature. To better illustrate the results, the fluid inlet velocity is increased to 1.5 m/s and 2 m/s. The outlet tem-

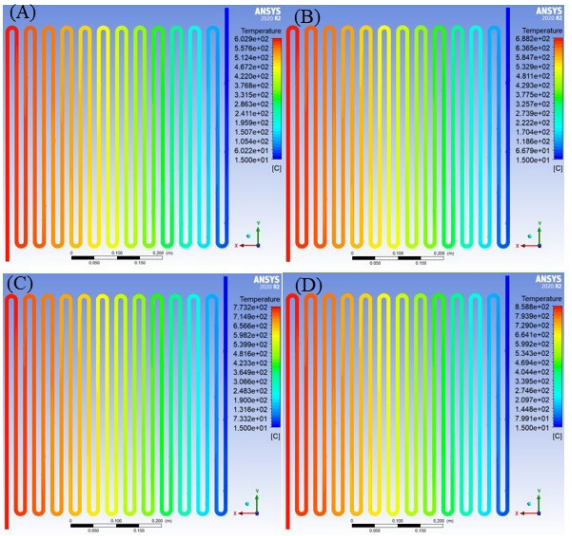

Figure 12. Static contours of temperature in the coil type heat exchanger for T_{in} = 15 °C and V_{wf} = 2 m/s: a) T_{cp} = 700 °C, b) T_{cp} = 800 °C, c) T_{cp} = 900 °C and d) T_{cp} = 1000 °C.

peratures were interpreted by changing the plate surface temperatures between 700 and 1000 °C. The corresponding temperature contours are given in Fig. 11 and Fig. 12. The effect of the increase in the fluid inlet velocity on the outlet temperature is clearly seen in the contours. When the plate surface temperature is constant at 1000 °C, it was seen that the outlet temperature, which was 804.9 °C at 1 m/s fluid inlet velocity, drops to 691.1 °C when the fluid inlet velocity is 1.5 m/s.

When the fluid inlet velocity is 2 m/s, it is seen that the outlet temperature drops significantly. It is seen that the outlet temperature, which is 565.6°C at 1 m/s fluid inlet velocity at a fixed plate surface temperature of 700°C, decreases by 25% and becomes 424.7°C when the fluid inlet velocity is doubled to 2 m/s. It is an excellent method to increase the fluid inlet velocity to obtain a more significant amount of steam. However, as seen in the results, increasing the fluid inlet velocity directly affects the outlet temperature. In this case, it is essential to design according to the desired output from the system. While the flow rate is kept low for high temperature steam, the system's flow rate can be reduced to obtain higher temperature steam.

This study clearly shows that the outlet temperature depends on the fluid inlet velocity and the plate surface temperature. This situation is comparatively demonstrated in Fig. 13. It is seen that increasing fluid inlet velocities decrease the outlet temperature at the same cast plate temperature. Similarly, for the same fluid inlet velocity, it is understood that increasing plate surface temperature raises the outlet temperature.

It can be said that when the fluid inlet velocity is constant, the outlet temperature increases linearly depending on the increasing plate surface temperature. However, high solar intensity is required for such high temperatures. This can happen in the middle of the day, which generally corresponds to noontime. The shortness of this period should be considered when installing the system in different regions.

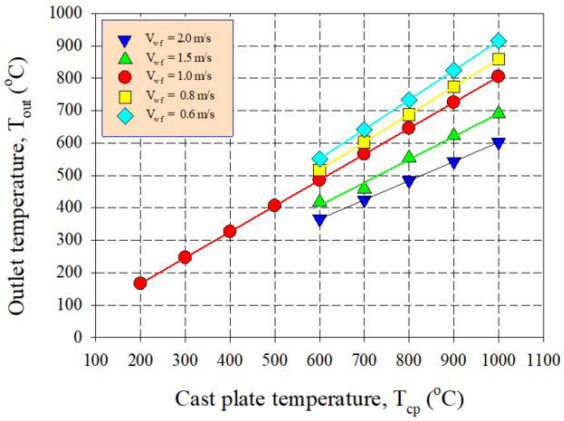

Figure 13. Outlet temperature of working fluid (T_out) as a function of cast plate temperature and working fluid velocity.

The preliminary performance testing of the novel design has been done for different sky conditions in the winter season of 2022 under cold climatic conditions in Bayburt, Turkey. For a totally cloudy sky conditions, the tests carried out using a 10-liter tank have revealed that the water temperature is 37.4 °C at the outlet of the heat exchanger after 2.5 hours operation time. For the said test, the absorber surface temperature has been reported to be in the range of 45-50 °C. when the sun is partially visible through the clouds for another 2.5 hours operation time, the water temperature reaches 74.4 °C with an absorber surface temperature of 85-90 °C. These experimental figures are also in accordance with the corresponding CFD results as shown in Fig. 14.

Another important output of the system is capacity. Increasing the fluid inlet velocity increases the flow rate and

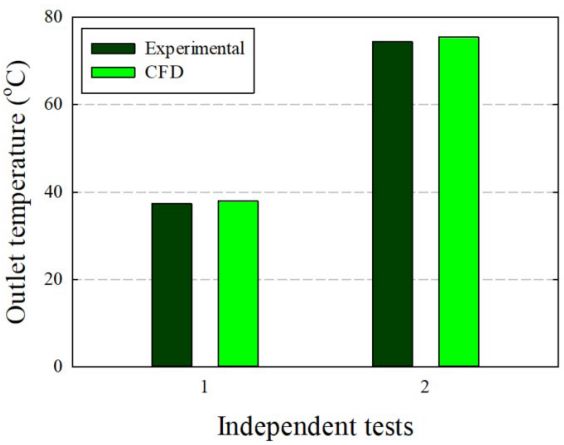

Figure 14. Comparison of experimental and CFD findings through water outlet temperature for different independents tests.

lowers the outlet temperature. In this case, there are differences in the system's capacity depending on operation time and inlet velocity. This situation is given comparatively in Fig. 15.

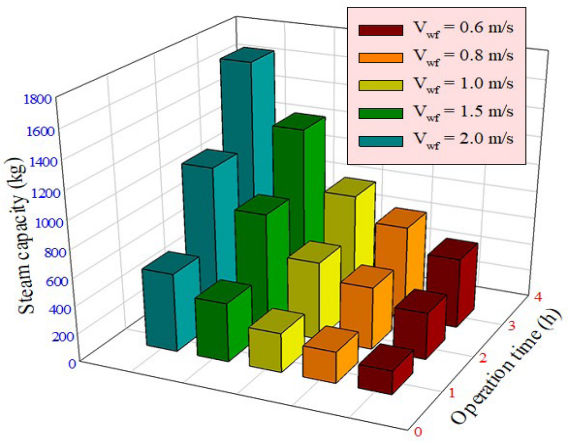

Figure 15. Steam capacity of the Fresnel lens driven novel hot water/steam generator as a function of operation time and velocity of working fluid.

When the graph is examined, it is seen that the operation time and capacity are linearly related for the same fluid inlet velocity. Similarly, the fluid inlet velocity can be increased to increase the capacity simultaneously.

The main point of the study is to obtain a high exit temperature from the heat exchangers by creating a surface at high temperatures with a fresnel lens. It also evaluates the relationship between the flow rate and the outlet temperature. For this reason, the figures are given separately, and the readers can examine them in detail. Temperature data for all velocities are collected in a single graph, providing faith in making multiple comparisons.

CONCLUSION

Thermal performance assessment of a Fresnel lens assisted hot water/steam generator is done through a CFD based numerical approach. The proposed unique system can be utilized for domestic and industrial purposes to meet hot water/steam demand at different capacities. A novel cast plate heat exchanger with copper coils is devised to benefit from concentrated solar power with maximum efficiency. For five different working fluid velocities (0.6, 0.8, 1.0, 1.5 and 2.0 m/s) and for four different cast plate temperatures (700, 800, 900 and 1000 °C), the outlet temperature of working fluid is achieved through a 3D CFD model. The capacity of the steam generator for different operating times (h = 1, 2 and 3 hours) is also investigated in the CFD analyses. The following bullet points can be concluded from the research:

The highest working fluid temperature at the outlet of heat exchanger is 914.8 °C for T_{cp} = 1000 °C and V_{wf} = 0.6 m/s.

The lowest temperature is obtained as 424.7 °C for T_{cp} = 700 °C and V_{wf} = 2.0 m/s.

The outlet temperature increases with increasing cast plate temperature, and decreases with the increasing working fluid velocity.

The maximum steam capacity of the proposed system for h = 3 hours and for V_{wf} = 2.0 m/s is 1696.5 kg.

The minimum steam capacity of the proposed system for h = 3 hours and for V_{wf} = 0.6 m/s is 508.9 kg.

The CR of the Fresnel lens utilized in the analyses is 100. The performance figures can be enhanced by utilizing concentrators with higher CRs.

The proposed system can work efficiently irrespective of changes in climatic parameters.

NOMENCLATURE

T_{cp}	cast plate temperature
T_{in}	inlet temperature
T_{out}	outlet temperature
V_{wf}	velocity of working fluid
Re	Reynolds number
V	velocity

GREEK LETTERS

μ	dynamic viscosity
ρ	density

ABBREVIATIONS

CFD	computational fluid dynamics
CR	concentration ratio
CSC	concentrated solar collector
HLC	heat loss coefficient
HRF	heat removal factor
PCM	phase change material

ACKNOWLEDGEMENTS

Erdem Cuce is grateful to Turkish Academy of Sciences (TÜBA) for their financial support to this research.

CONFLICT OF INTEREST

Authors approve that to the best of their knowledge, there is not any conflict of interest or common interest with an institution/organization or a person that may affect the review process of the paper.

AUTHOR CONTRIBUTION

All authors contributed equally to the submission of our article for consideration in the Hittite Journal of Science and Engineering.

REFERENCES

1. Verma S, Verma A, Kumar V, Gangil B. Concentrated photovoltaic thermal systems using Fresnel lenses-A review. Mater Today Proc 2020;44:4256–doi:10.1016/j.matpr.2020.10.542.
2. Bellos E, Skaltsas I, Pliakos O, Tzivanidis C. Energy and financial investigation of a cogeneration system based on linear Fresnel reflectors. Energy Convers Manag 2019;198. doi:10.1016/j.enconman.2019.111821.
3. Bellos E, Tzivanidis C. Alternative designs of parabolic trough solar collectors. Prog Energy Combust Sci 2019;71:81–117.doi:10.1016/j. pecs.2018.11.001.
4. Bellos E. Progress in the design and the applications of linear Fresnel reflectors – A critical review. Therm Sci Eng Prog 2019;10:112–doi:10.1016/j.tsep.2019.01.014.
5. Zhai H, Dai YJ, Wu JY, Wang RZ, Zhang LY. Experimental investigation and analysis on a concentrating solar collector using linear Fresnel lens. Energy Convers Manag 2010;51:48–55.doi:10.1016/j.enconman.2009.08.018.
6. Perini S, Tonnellier X, King P, Sansom C. Theoretical and experimental analysis of an innovative dual-axis tracking linear Fresnel lenses concentrated solar thermal collector. Sol Energy 2017;153:679–90. doi:10.1016/j. solener.2017.06.010.
7. Ma X, Zheng H, Tian M. Optimize the shape of curved-Fresnel lens to maximize its transmittance. Sol Energy 2016;127:285–9 doi:10.1016/j.solener.2016.01.014.
8. Lin M, Sumathy K, Dai YJ, Zhao XK. Performance investigation on a linear Fresnel lens solar collector using cavity receiver. Sol Energy 2014;107:50–62.doi:10.1016/j.solener.2014.05.026.
9. Xie WT, Dai YJ, Wang RZ. Thermal performance analysis of a line-focus Fresnel lens solar collector using different cavity receivers. Sol Energy 2013;91:242–55. doi:10.1016/j. solener.2013.01.029.
10. Wu G, Zheng H, Ma X, Kutlu C, Su Y. Experimental investigation of a multi-stage humidification-dehumidification desalination system heated directly by a cylindrical Fresnel lens solar concentrator. Energy Convers Manag 2017;143:241–doi:10.1016/j.enconman.2017.04.011.
11. Beltagy H, Semmar D, Lehaut C, Said N. Theoretical and experimental performance analysis of a Fresnel type solar concentrator. Renew Energy 2017;101:782–93. doi:10.1016/j. renene.2016.09.038.
12. Asrori A, Suparman S, Wahyudi S, Widhiyanuriyawan D. Investigation of Steam Generation Performance on Conical Cavity Receiver By Different Geometric Concentration Ratios for Fresnel Lens Solar Concentrator. Eastern-European J Enterp Technol 2020;4:6–14. doi:10.15587/1729-4061.2020.209778.
13. Sanchez Vega LR. Modeling and experimental evaluation of a small-scale fresnel solar concentrator system. Renewables Wind Water, Sol 2016;3. doi:10.1186/s40807-016-0021-9.
14. Zulkifle I, Ruslan MHH, Othman MYH, Ibarahim Z. Analytical analysis of solar thermal collector with glass and Fresnel lens glazing. AIP Conf Proc 2018;1940. doi:10.1063/1.5027920.
15. Ma X, Zheng H, Liu S. Optimization on a cylindrical Fresnel lens and its validation in a medium-temperature solar steam generation system. Renew Energy 2019; 134:1332-43.
16. ANSYS FLUENT. Fluid Simulation Software.
17. Cengel, Y. A., & Ghajar, A. J. (2014). Heat and mass transfer: Fundamentals and applications (5th ed.). McGraw-Hill Professional.
18. Arslan, M. Igci, A. Thermal performance of a vertical solar hot water storage tank with a mantle heat exchanger depending on the discharging operation parameters. Solar Energy, 2015;116;184-204.